



# Purification and economic analysis of nanoclay from bentonite

Zahra Biglari Quchan Atigh<sup>1</sup> · Ava Heidari<sup>1</sup> · Alireza Karimi<sup>2</sup> · Mohammad Ali Pezhman<sup>3</sup> · Behnam Asgari Lajayer<sup>4</sup> · Eder Claudio Lima<sup>5</sup>

Received: 28 March 2020 / Accepted: 9 November 2020 / Published online: 15 November 2020  
© Springer-Verlag GmbH Germany, part of Springer Nature 2020

## Abstract

Nowadays, due to the most application of montmorillonite, its purification from raw bentonite has great importance. More than 76% of bentonite is composed of montmorillonite, and its industrial applications are related to its montmorillonite content. In this study, the nanoclay was extracted from bentonite by the use of centrifugal force. The results of the field-emission scanning electron microscopy (FE-SEM) analysis show that the nanosized of purified montmorillonite has a sheet structure with a spacing of 22.41 nm and 45.0 nm. The sharp peaks in X-ray diffraction analysis (XRD) illustrated that the montmorillonite purified successfully, and the results of Fourier-transform infrared spectrophotometry (FT-IR) revealed the successful incorporation of the metabolic extraction within the montmorillonite. By comparison of Brunauer–Emmett–Teller (BET) results with IUPAC, it can be realized that the synthesized montmorillonite nanoclay has a microporous structure (< 2 nm) with a surface area of 11.325 m<sup>2</sup> g<sup>-1</sup>. According to IUPAC classification, the BET isotherms of montmorillonite and bentonite indicate a hysteresis loop belonging to the type H3. Finally, the economic analysis results revealed to this method could be the best option for achieving high purity montmorillonite for future applications.

**Keywords** Purification · Nanoclay · Montmorillonite · Bentonite · Cost analysis

## Introduction

In recent decades, the use of natural bentonites for different approaches has been considered significantly due to their unique structure, low-cost, thermal stability, high immunity, high exchange capacity, and interactions with materials (Chilhi et al. 2019; Yadav et al. 2019). Soil mineral smectite in

bentonite with aluminum octagonal sheets is located between the tetrahedral silica sheets (Awad et al. 2019). These layers of material with a unique structure are the best option for designing and preparing green catalysts (Bananezhad et al. 2019). Inorganic bentonite is composed of clay or pseudo-clay family and swollen minerals. The term bentonite was first used for clays with colloidal plastic properties in the Cretaceous sediments of the Wyoming region (Inglethorpe et al. 1993). Today, the term bentonite is used in clays that are rich in montmorillonite regardless of their origin (Inglethorpe et al. 1993). The economical use of bentonite depends on the amount of mineral montmorillonite, which contains 60 to 70% of bentonite (Krupskaya et al. 2017). According to its exchangeable cations, bentonite is classified as either calcium bentonite or sodium bentonite. Also, the terms expandable and non-expandable clay is synonymous with this group (Nadziakiewicz et al. 2019; Leal et al. 2019). Recently, montmorillonite purification from bentonite has been reported (Qiao et al. 2020; Gong et al. 2020). The particular structure of montmorillonite clay has led to numerous applications. It is used as a catalyst, an antibacterial agent in the pharmaceutical industry (Porebska et al. 2020), and an adsorbent for water purification (Keymirov 2018).

Furthermore, due to its ease in purification, it was used as an effective adsorbent to remove pollutants (Wang and Zhuang

---

Responsible Editor: Philippe Garrigues

✉ Zahra Biglari Quchan Atigh  
zahrabiglari39@yahoo.com

✉ Behnam Asgari Lajayer  
asgarihemayat@gmail.com

<sup>1</sup> Department of Environmental Science, Faculty of Natural Resource and Environment, Ferdowsi University of Mashhad, Mashhad, Iran

<sup>2</sup> Department of Soil Science, Faculty of Agriculture, Ferdowsi University of Mashhad, Mashhad, Iran

<sup>3</sup> Department of Chemical Engineering, Faculty of Engineering, Ferdowsi University of Mashhad, Mashhad, Iran

<sup>4</sup> Health and Environment Research Center, Tabriz University of Medical Sciences, Tabriz, Iran

<sup>5</sup> Institute of Chemistry, Federal University of Rio Grande do Sul, Porto Alegre, RS, Brazil

2017). The most commonly used bentonite for industrial use is high purity white bentonite with a cation exchangeability of at least about 60% of the equivalent cations; impurities will have adverse effects on bentonite quality and its potential applications (Morais et al. 2020). Therefore, unnecessary bentonite impurities should be removed as much as possible. Different methods have been used to achieve high purity montmorillonite with a particle size of smaller than 2  $\mu\text{m}$ , including sieving, particle dispersion based on Stokes law, and the use of ultrasonic magnetic dispersion for pure montmorillonite (Thuc et al. 2010; Barakan and Aghazadeh 2019; Thuc et al. 2010; Liu et al. 2012; Veiskarami et al. 2017).

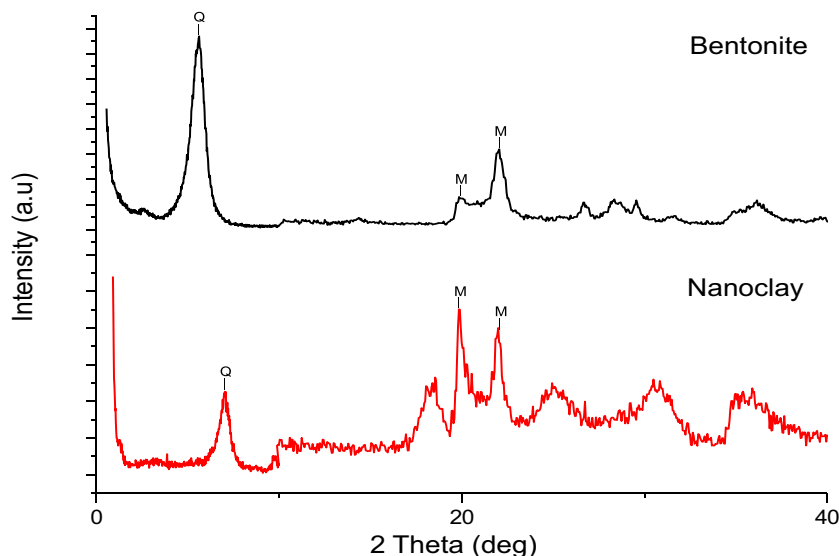
In this study, montmorillonite purified from bentonite and characterized by Fourier-transform infrared spectrophotometry (FT-IR), X-ray diffraction analysis (XRD), field-emission scanning electron microscopy (FE-SEM), and Brunauer–Emmett–Teller (BET) methods. Besides, economic analysis for purification of montmorillonite from bentonite investigated based on industrial scale. As mentioned above, in the past research, bentonite has been applied without purification, which to this research, the capabilities of purified montmorillonite are illustrated with characterization. Moreover, economic analysis will inspire various applications in the future.

## Material and method

### Materials

Natural bentonite was obtained from the Qayen mine in eastern Iran. Sodium hexametaphosphate ( $\text{NaPO}_3$ )<sub>6</sub>, sodium carbonate ( $\text{Na}_2\text{CO}_3$ , 98.5%), sodium chloride ( $\text{NaCl}$ , 99.5%), and hydrochloric acid (37.0%) were purchased from Merck (Darmstadt, Germany).

**Fig. 1** X-ray diffraction of bentonite and nanoclay



### Clay purification and extraction

The soil content of raw bentonite included clay (80%) and silt (20%). The basal spacing of montmorillonite is 7.94 Å. Its chemical composition was found to be as follows:  $\text{SiO}_2$  63.7%,  $\text{Al}_2\text{O}_3$  12.2%,  $\text{Fe}_2\text{O}_3$  2.4%,  $\text{CaO}$  3.7%,  $\text{Mg}$  1.9%,  $\text{Na}_2\text{O}$  1.7%,  $\text{K}_2\text{O}$  0.6%,  $\text{SO}_3$  0.4%,  $\text{P}_2\text{O}_5$  < 0.1%,  $\text{TiO}_2$  0.3%,  $\text{Cl}$  0.4%, and L.O.I 12.43%. For purification, the crushed bentonite sample was sieved by a 325 mesh and then placed into an electronic furnace at 350 °C to remove the organic matter (Calabi-Floody et al. 2011). Then, 50 g of bentonite was slurried in 100 mL 1 M HCl and washed twice with deionized water. Finally, to extract clay from the sample matrix, it dispersed in 2.5 L of distilled water containing 0.9 g sodium hexametaphosphate and 0.2 g sodium carbonate and centrifuged for 15 min at 4000 rpm at room temperature. Afterward, the aqueous fraction was collected, and the obtained clay was dried at 70 °C for 24 h.

### Nanoclay extraction

The nanoclay was separated from clay fraction using the method described in the literature (Calabi-Floody et al. 2011). First, 5 g of the obtained clay was slurried in 300 mL of 1 M NaCl and centrifuged for 43 min at 8000 rpm at room temperature. In this stage, the centrifuge speed was similar to the method (Li and Hu 2003), and the diameter of particles was less than 100 nm. The first aqueous fraction was discarded after centrifugation to remove the mineral impurities. The solid fraction was slurried in 50 mL water with a moderate stirring for 40 min and again centrifuged at 8000 rpm. The aqueous phase was collected while the solid fraction was slurried again in water and re-centrifuged. This step was repeated 11 times, and finally, the collected supernatant that contained nanoclay was dialyzed (1000 kDa

**Fig. 2** The FT-IR spectra of bentonite and nanoclay

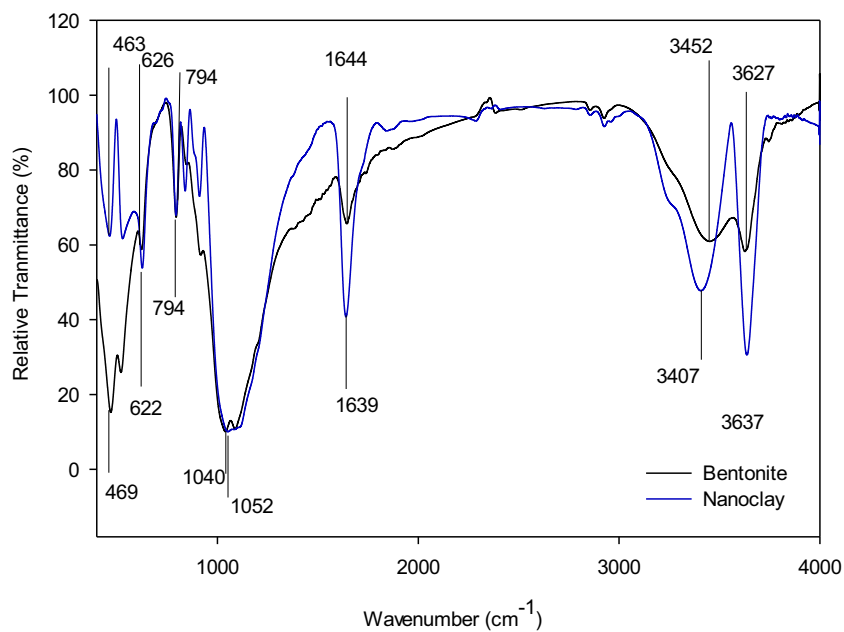


**Fig. 3** a–d Field-emission scanning electron microscopy (FE-SEM) images revealing sheets of nanoclay (a, b) and bentonite (c, d)

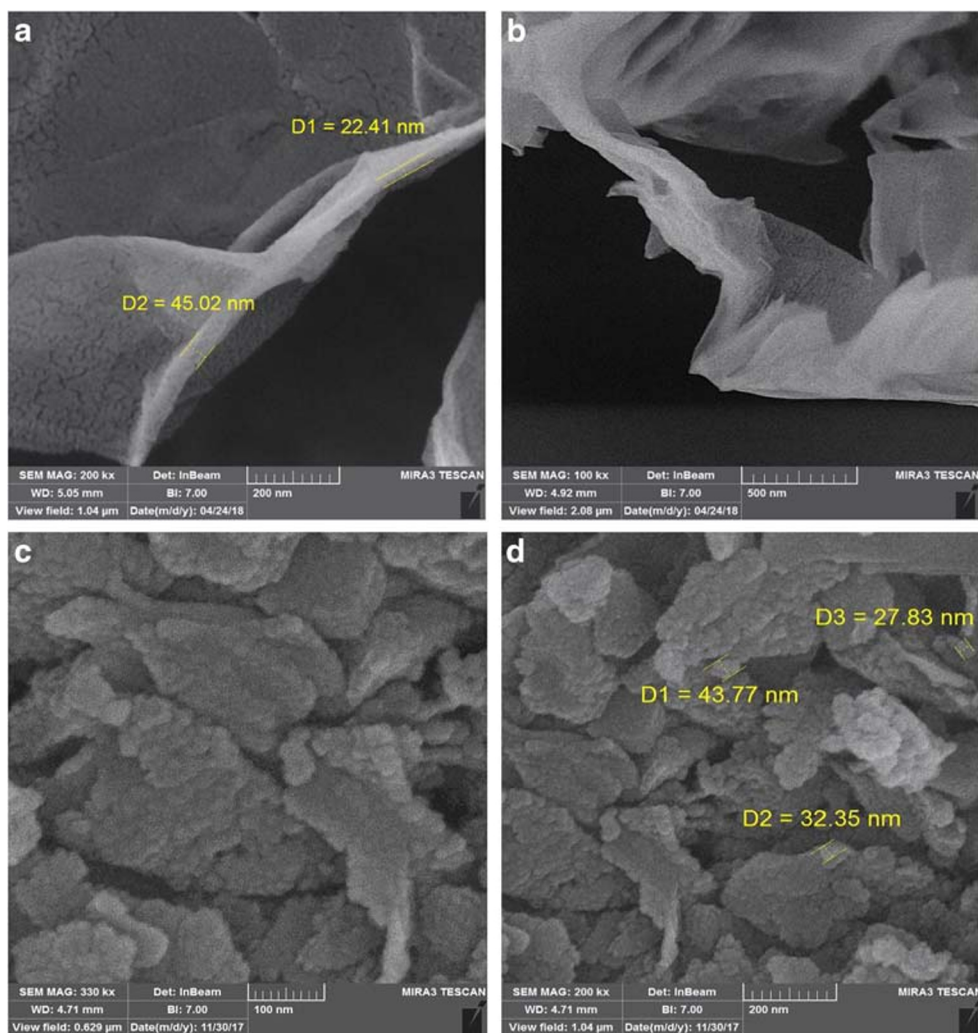


**Table 1** Structure parameters of the nanoclay and bentonite

Sample name	Average pore diameter (nm)	A <sub>BET</sub> (m <sup>2</sup> /g) BET (surface area)	Total pore volume (cm <sup>3</sup> (STP) g <sup>-1</sup> )	Average nanopore diameter (nm) BJH method
Bentonite	13.74	46.326	0.159	1.29
Nanoclay	16.92	11.325	0.047	1.29

membrane) using distilled water until the conductivity of the water achieved 0.5–0.8 μS cm<sup>-1</sup> (Calabi-Floody et al. 2011).

### Characterization

The crystal structure of bentonite and the obtained nanoclay was determined by the X-ray powder diffraction (XRD) technique (PW1730, PHILIPS Mark, and Holland). The functional groups of bentonite and nanoclay were detected using a Nicolet 6700 FT-IR spectrometer (Thermo Scientific, AVATAR, American) in the range of 400 to 4000 cm<sup>-1</sup>. The surface morphology of the bentonite and nanoclay was carried out using a field-emission gun scanning electron microscope (FE-SEM) (TEACAN, MIRA III, Czech Republic) at an accelerating voltage 5 kV for 20, 50, 100, 200 nm, and 1 μm. The nanoclay samples were slurried in water (1 μg mL<sup>-1</sup>) (Calabi-Floody et al. 2011). The nanoparticles' surface area was measured by an ASAP 2010 analyzer from Micrometrics Instrument Corporation.

## Results and discussion

### XRD analysis

The XRD analysis of bentonite and nanoclay is depicted in Fig. 1. It is clear that the peaks of bentonite started from 2θ = 11.09 with *d*-spacing 7.97 Å and ended at 2θ = 40.0 with *d*-

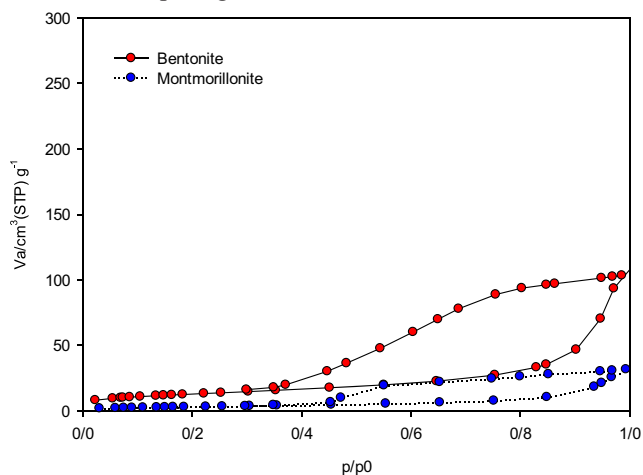


**Fig. 4** The plot of AdsDes bentonite and nanoclay

**Table 2** Estimated capital cost for nanoclay form bentonite

Equipment	Cost (\$)
Centrifuge	900
Oven	700
Stirrer (2 devices)	400
Total equipment cost	2000
Equipment installation \$ contingency	200
Instrumentation	750
Total capital costs	2950

spacing 1.42 Å. Its peaks are located at 2θ: 19.80, 22.4, 28.44, 31.53, 34.73, 36.35; on the other hand, the peaks of nanoclay started at 2θ = 18.52, *d*-spacing 4.79 Å, and ended at 2θ = 36.20, *d*-spacing 2.48 Å. The identified patterns contain silicon oxide (SiO<sub>2</sub>) and sodium-magnesium-aluminum silicate hydroxide hydrate (Na<sub>0.3</sub>(Al, Mg)<sub>2</sub>Si<sub>4</sub>O<sub>10</sub>(O·H)<sub>2</sub>·4H<sub>2</sub>O) with the displacements 0.000 and 0.464° (2<sup>θ</sup>) in the nanoclay, respectively. The reference codes, 98-003-5568, 98-006-0915, 98-005-5990, and 00-013-0230, located at 2θ = 19.86, 21.94, 30.58, and 36.2, represent low quartz, low cristobalite, sodium ozonide, and magnesium silicate, respectively in montmorillonite nanoclay.

### Fourier-transform infrared spectroscopy

The FT-IR spectra of bentonite and nanoclay are illustrated in Fig. 2. The peak, at near 3434 cm<sup>-1</sup>, is related to the stretching vibration of O–H groups of adsorbed water molecules (Slavutsky et al. 2012). The peak at 1644 cm<sup>-1</sup> represents the deformation of the O–H group of water. The attendance of sharp peaks at 1050 cm<sup>-1</sup> and 794 cm<sup>-1</sup> shows Si–O and Al–Fe–OH groups, respectively, and the peak at 621 cm<sup>-1</sup> is attributed to the stretching vibration of the Al–O bond. Finally, the intense peaks at around 475 cm<sup>-1</sup> are related to the stretching vibrations of Si–O–Si (tetrahedral) and Si–O–Si (amorphous) groups (Saha et al. 2004; Wu et al. 2016).

**Table 3** Annual operating costs for nanoclay from bentonite

Item	Annual cost (\$)
Bentonite	5.25
Hexametaphosphate sodium	200
NaCO <sub>3</sub>	200
HCL	100
H <sub>2</sub> O	100
NaCl	200
Characterization	1800
Packing and contingency	220



**Table 4** Summary of costs for purification of nanoclay from bentonite

Purchased equipment cost	2000\$
Capital cost	2950\$
Total fixed capital investment	3300\$
Total annual operating cost	1980\$
Estimated annual production of nanoclay (g)	12,000\$
Estimated cost for nanoclay from bentonite	0.275\$ per g

### FE-SEM analysis

The results of the field-emission scanning electron microscopy (FE-SEM) results for bentonite and nanoclay show the presence of micro- and mesoporous structure. The results show that the obtained nanoclay is similar to the montmorillonite structure (Issaabadi et al. 2017) and contained several arrays of cleaved sheets (Khedr et al. 2006). According to Fig. 3, the nanoclay has particle sizes of 200 and 500 nm; however, bentonite has particle sizes of 100 and 200 nm.

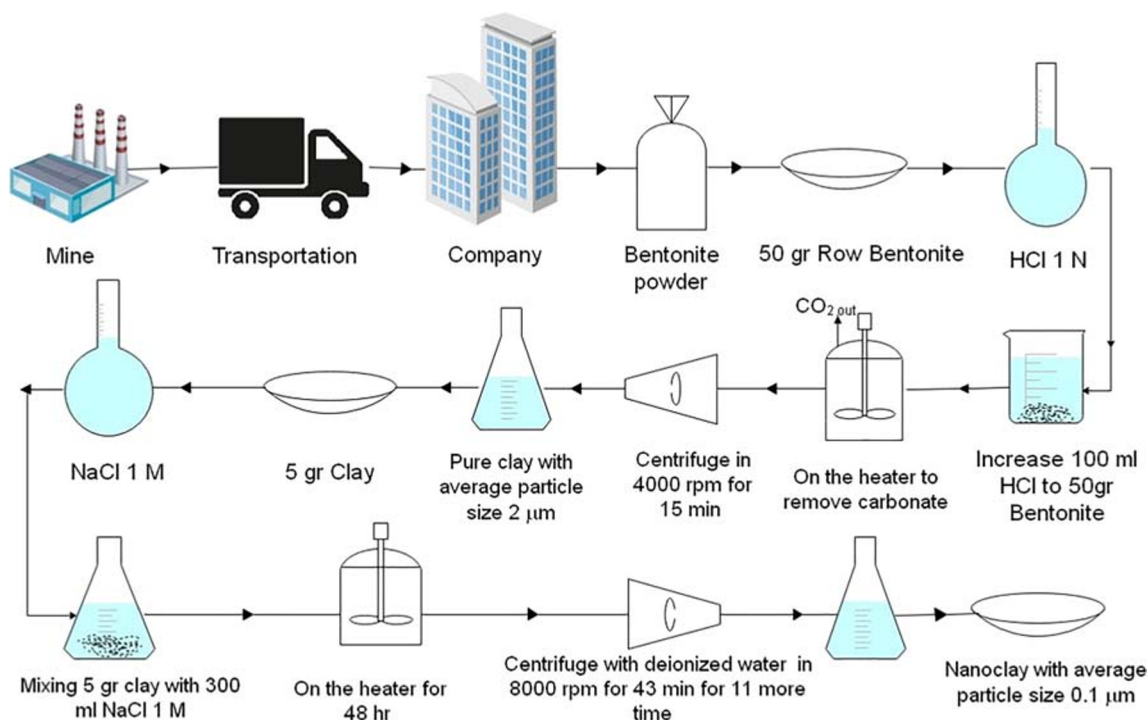
### Specific surface area and pore size distribution

The BET surface area was measured by nitrogen isotherm by BET equation in  $N_2$  adsorption–desorption at the temperature 77 K in the relative pressure range from 0.5 to 0.06  $p/p_0$  for clay and nanoclay (Hayati-Ashtiani 2011). Also, the mean pore diameter was obtained by the BJH method. Table 1 illustrates the BET surface area and average pore diameter for

clay and montmorillonite. As could be seen, according to the BJH analysis, montmorillonite and bentonite have an average pore diameter of 1.29 nm, and the total pore volume for bentonite and montmorillonite were 0.159 and 0.047  $cm^3 g^{-1}$ , respectively. The BET analysis shows that bentonite and montmorillonite's surface area was 46.326 and 11.325  $m^2 g^{-1}$ , respectively, and the average pore diameter for bentonite and montmorillonite was 13.74 and 16.92 nm, respectively. The information of  $N_2$  adsorption–desorption isotherms for nanoclay is depicted in Fig. 4. For montmorillonite as the main constituent of clay,  $N_2$  can coat the other primary surface area, but not the interlamellar space, as shown by small surface areas obtained by this technique. Conforming to the International Union of Pure and Applied Chemistry (IUPAC), pores sizes are as classified to (Alhamami et al. 2014) macropore, mesoporous, and micropore with the sizes of > 50 nm, 2–50 nm, and < 2 nm, respectively. The BET isotherms of montmorillonite and bentonite indicate a hysteresis loop belonging to the type  $H_3$  according to IUPAC classification (Yoon et al. 2010; Yadav et al. 2018).

### Cost analysis

The nanoclay cost analysis was predicated on the natural, low-cost bentonite via a high prospective and effectual method. Therefore, an economic assessment was implemented for defining the construction cost based on industrial-scale experiences and its extrapolation to a real experience of producing it on a large scale. Moreover, the diagram for scaling up the

**Fig. 5** Process flow diagram for the production of nanoclay

construction procedure is explained in Fig. 5. Generally, this research put out accurate data on the proximate assessment of estimated capital cost, annual operational costs, and summary of costs for purification nanoclay from bentonite exposed in Tables 2, 3, and 4, respectively. As can be seen, separating montmorillonite from bentonite, there is a low-cost procedure. Furthermore, the cost of purification was spent on consumed materials such as distilled water, hydrochloric acid, and sodium carbonate.

This research provides completed data on the proximate assessment of annual operating costs and capital costs for purifying nanoclay from bentonite. Consequently, it is considered an underestimated yield of 9% for the production of nanoclay from bentonite in which feasibility is ensured, and then, the cost estimation was obtained for 300 days/year and a personnel size of 2 people per shift (one shift) for 24 h/day. Besides, it is guesstimated that \$ 0.275 be needed for manufacturing 1 g of nanoclay from bentonite. Today, different methods of purification of bentonite are used throughout the world. The most critical factor in choosing the purification method is economic factors. In Iran, bentonite is used without any purification (Modabberi et al. 2015). Bentonite mining conditions in Iran and the challenges associated with exporting this mineral to other countries and other factors, including the economic costs associated with processing this mineral, led us to take a small step toward improving and resolving this problem.

## Conclusion

The purpose of the proposed paper is to extract the nanoclay from raw bentonite using centrifugal force. The obtained nanoclay was characterized by XRD, BET, FE-SEM, and FT-IR analyses. The FE-SEM analysis results show that the obtained nanoclay has a sheet structure with a 22.41 nm and 45.0 nm spacing. The surface area for bentonite and montmorillonite was 46.326 and 11.325 m<sup>2</sup> g<sup>-1</sup>, respectively, and the average pore diameter for bentonite and montmorillonite was 13.74 and 16.92 nm, respectively. The BET isotherms of montmorillonite and bentonite indicate a hysteresis loop belonging to the type H3 according to IUPAC classification; finally, the economic analysis of the proposed purification technique showed that the mineral was synthesized and purified economically and could be used for various applications such as removing contaminants from the environment.

**Authors' contributions** Zahra Biglari Quchan Atigh: Conducted experimental verification, analyzed the data, and wrote the manuscript

Ava Heidari: Contributed to the research idea and designed the study

Alireza Karimi: Contributed to the conception of the study

Mohammad Ali Pezhman: Helped the cost analysis through constructive discussions

Behnam Asgari Lajayer: Prepared, edited, and submitted the manuscript

Eder Claudio Lima: Helped perform the analysis with constructive discussions and revised the article

**Funding** Financial support and sponsorship from the Foundation for Research Support of the State of Rio Grande do Sul (FAPERGS), National Council for Scientific and Technological Development (CNPq, Brazil), and Coordination of Improvement of Higher Education Personnel (CAPES, Brazil) are acknowledged.

**Data availability** The datasets used or analyzed during the current study are available from the corresponding author on reasonable request.

## Compliance with ethical standards

**Conflict of interest** The authors declare that they have no conflict of interest.

**Ethical approval** Not applicable.

**Consent to participate** Not applicable.

**Consent to publish** Not applicable.

## References

- Alhamami M, Doan H, Cheng CH (2014) A review on breathing behaviors of metal-organic-frameworks (MOFs) for gas adsorption. *Materials* 7:3198–3250. <https://doi.org/10.3390/ma7043198>
- Awad AM, Shaikh SMR, Jalab R, Gulied MH, Nasser MS, Benamor A, Adham S (2019) Adsorption of organic pollutants by natural and modified clays: a comprehensive review. *Sep Purif Technol* 228: 115719. <https://doi.org/10.1016/j.seppur.2019.115719>
- Bananezhad B, Islami MR, Ghonchehpour E, Mostafavi H, Tikdari AM, Rafei HR (2019) Bentonite clay as an efficient substrate for the synthesis of the super stable and recoverable magnetic nanocomposite of palladium (Fe<sub>3</sub>O<sub>4</sub>/Bentonite-Pd). *Polyhedron* 162:192–200. <https://doi.org/10.1016/j.poly.2019.01.054>
- Barakan S, Aghazadeh V (2019) Separation and characterization of montmorillonite from low-grade natural bentonite: using a non-destructive method. *Micro & Nano Lett* 14:688–693. <https://doi.org/10.1049/mnl.2018.5364>
- Calabi-Floody M, Bendall JS, Jara AA, Welland ME, Theng BKG, Rumpel C, Mora M d l L (2011) Nanoclays from an Andisol: extraction, properties, and carbon stabilization. *Geoderma* 161:159–167. <https://doi.org/10.1016/j.geoderma.2010.12.013>
- Chihi R, Bliidi I, Trabelsi-Ayadi M, Ayari F (2019) Elaboration and characterization of a low-cost porous ceramic support from natural Tunisian bentonite clay. *Comptes Rendus Chimie, Second International Symposium Clays and Ceramics for Environmental Applications* 22:188–197. <https://doi.org/10.1016/j.crci.2018.12.002>
- Gong Z, Liao L, Lu G, Wand X (2020) A simple method for physical purification of bentonite. *Appl Clay Sci* 119:294–300. <https://doi.org/10.1016/j.clay.2015.10.031>
- Hayati-Ashtiani M (2011) Characterization of nano-porous bentonite (montmorillonite) particles using FTIR and BET-BJH analyses. *Part Part Syst Charact* 28:71–76. <https://doi.org/10.1002/ppsc.201100030>

- Inglethorpe SBJ, Morgan DJ, Highley DE, Bloodworth AJ (1993) Technical report WG/93/20. Mineralogy and petrology Series. British Geology Survey. 1–115
- Issaabadi Z, Nasrollahzadeh M, Sajadi SM (2017) Green synthesis of the copper nanoparticles supported on bentonite and investigation of its catalytic activity. *J Clean Prod* 142:3584–3591. <https://doi.org/10.1016/j.jclepro.2016.10.109>
- Keymirov MA (2018) Water purification of ions of heavy metals by montmorillonite modified with polyamine. *J Water Chem Technol* 40:320–326. <https://doi.org/10.3103/S1063455X18060024>
- Khedr MH, Omar AA, Abdel-Moaty SA (2006) Reduction of carbon dioxide into carbon by freshly reduced CoFe<sub>2</sub>O<sub>4</sub> nanoparticles. *Mater Sci Eng A* 432:26–33. <https://doi.org/10.1016/j.msea.2006.06.012>
- Krupskaya V, Zakusin S, Tyupina E, Dorzhieva O, Zhukhlistov A, Belousov P, Timofeeva M (2017) Experimental study of montmorillonite structure and transformation of its properties under treatment with inorganic acid solutions. *Minerals* 7:49. <https://doi.org/10.3390/min7040049>
- Leal CA, Brunet MNC, Amorim LV, Lira HL, Nogueira FCC, Costa WRP (2019) Influence of reactivity and mineralogical composition on instability due to the disintegration of shales from Paraíba and Ceará States, Brazil. *Cerâmica* 65:400–406. <https://doi.org/10.1590/0366-69132019653752630>
- Li Z, Hu N (2003) Direct electrochemistry of heme proteins in their layer-by-layer films with clay nanoparticles. *J Electroanal Chem* 558:155–165. [https://doi.org/10.1016/S0022-0728\(03\)00390-5](https://doi.org/10.1016/S0022-0728(03)00390-5)
- Liu XD, Lu XJ, Qiu J, Wang ZM, Wu P (2012) Purification of low-grade Ca-bentonite for iron ore pellets. *AMR* 454:237–241. <https://doi.org/10.4028/scientific5/AMR.454.237>
- Modabberi S, Namayandeh S, López-Galindo A, Viseras C, Setti M, Ranjbaran M (2015) Characterization of Iranian bentonites to be used as pharmaceutical materials. *Appl Clay Sci* 116–117:193–201
- Morais ICG, Silva IA, Buriti BMB, Fernandes JV, Silva DS, Neves GA, Ferreira HS (2020) Influence of the addition process on cation exchange capacity and viscosity of bentonitic clay dispersions. *Cerâmica* 66:81–87. <https://doi.org/10.1590/0366-69132020663772695>
- Nadziakiewicz M, Kehoe S, Micek P (2019) Physico-chemical properties of clay minerals and their use as a health promoting feed additive *Animals (Basel)* 9. <https://doi.org/10.3390/ani9100714>
- Porebska R, Rybak A, Rapacz-Kmita A (2020) Montmorillonite–triclosan hybrid as effective antibacterial additive with enhanced thermal stability for protection of plastic electrical components. *Polym Bull* 77:17–31. <https://doi.org/10.1007/s00289-019-02699-x>
- Qiao Z, Liu Z, Zhang S, Yang Y, Wu Y, Liu L, Liu Q (2020) Purification of montmorillonite and the influence of the purification method on textural properties. *Appl Clay Sci* 187:105491. <https://doi.org/10.1016/j.clay.2020.105491>
- Saha UK, Liu, C, Kozak, LM, Huang, PM (2004) Kinetics of selenite adsorption on hydroxy aluminum- and hydroxy aluminosilicate-montmorillonite complexes. *Soil Sci Soc Am J*
- Slavutsky AM, Bertuzzi MA, Armada M (2012) Water barrier properties of starch-clay nanocomposite films. *Braz J Food Technol* 15:208–218. <https://doi.org/10.1590/S1981-67232012005000014>
- Thuc CNH, Grillet AC, Reinert L, Ohashi F, Thuc HH, Duclaux L (2010) Separation and purification of montmorillonite and polyethylene oxide modified montmorillonite from Vietnamese bentonites. *Appl Clay Sci* 49:229–238. <https://doi.org/10.1016/j.clay.2010.05.011>
- Veiskarami M, Mansouri Esfahani M, Nasiri Sarvi M (2017) Qualification of the montmorillonite purification process for nanoclay production. *Iran J Crystallogr Mineral* 25:557–566. <https://doi.org/10.18869/acadpub.ijcm.25.3.557>
- Wang J, Zhuang S (2017) Removal of various pollutants from water and wastewater by modified chitosan adsorbents. *Crit Rev Environ Sci Technol* 47:2331–2386. <https://doi.org/10.1080/10643389.2017.1421845>
- Wu H, Xie H, He G, Guan Y, Zhang Y (2016) Effects of the pH and anions on the adsorption of tetracycline on iron-montmorillonite. *Appl Clay Sci* 119:161–169. <https://doi.org/10.1016/j.clay.2015.08.001>
- Yadav VB, Gadi R, Kalra S (2018) Synthesis and characterization of novel nanocomposite using kaolinite and carbon nanotubes. *Appl Clay Sci* 155:30–36
- Yadav VB, Gadi R, Kalra S (2019) Clay-based nanocomposites for removal of heavy metals from water: a review. *J Environ Manag* 232: 803–817. <https://doi.org/10.1016/j.jenvman.2018.11.120>
- Yoon JW, Seo YK, Hwang YK, Chang JS, Leclerc H, Wuttke S, Bazin P, Vimont A, Daturi M, Bloch E, Llewellyn PL, Serre C, Horcajada P, Grenèche JM, Rodrigues AE, Férey G (2010) Controlled reducibility of a metal-organic framework with coordinatively unsaturated sites for preferential gas sorption. *Angew Chem Int Ed* 49:5949–5952. <https://doi.org/10.1002/anie.201001230>

**Publisher's note** Springer Nature remains neutral with regard to jurisdictional claims in published maps and institutional affiliations.